Experimental Thermal and Fluid Science 108 (2019) 55–60

Contents lists available at ScienceDirect

Experimental Thermal and Fluid Science

journal homepage: www.elsevier.com/locate/etfs

Accessing quantitative heat transfer with Temperature Decline Thermography

Stefan von Hoesslin[a,*], Juergen Gruendmayer[a], Andreas Zeisberger[a], Christian J. Kähler[b]

[a] MTU Aero Engines AG, Dachauer Str. 665, 80995 Munich, Germany
[b] Universität der Bundeswehr, Institute of Fluid Mechanics and Aerodynamics, Werner-Heisenberg-Weg 39, 85577 Neubiberg, Germany

A B S T R A C T

Analyzing local heat transfer on complex components in fluid flows is crucial for the optimization of modern aerodynamical systems. Many flow situations like in gas turbines, are difficult to access and require fast measurement techniques which offer two-dimensional information with negligible impact on flow conditions. Therefore, a transient measurement technique based on infrared thermography is investigated to access local heat transfer coefficients without contact by means of a calibration. A flat plate in a free-jet is used as a calibration vehicle where results are compared to the flat plate Nusselt correlation in laminar flow. To transfer the observed linear calibration relation to different flow conditions, a turbulent boundary layer is generated and results are compared to the turbulent Nusselt correlation. Good agreement of converted measurement data and theory is obtained. Temperature Decline Thermography (TDT) was introduced by the authors to qualitatively measure laminar-turbulent transition. In this work TDT is extended to access quantitative heat transfer coefficients.

1. Introduction

For the design of modern aerodynamical systems with highest possible efficiencies, it is desirable to gain detailed knowledge about laminar-turbulent transition and heat transfer distribution of flows around complex aerodynamical components. Many available measurement techniques, like for example surface hot films, access this information with great effort of instrumentation and calibration. For fast rotating devices like turbines, most techniques are impractical which is why a method based on infrared thermography was introduced recently by the authors [25,24]. It has been shown that Temperature Decline Thermography (TDT) can be used for the qualitative visualization of laminar-turbulent transition in boundary layers and will now be investigated for the possibility of deriving quantitative heat transfer coefficients from recorded data.

A classification of techniques for measuring convective heat transfer is proposed in the literature [19,1,6]. Heat flux sensors often consist of one or more thin metal films or foils mounted on a bulk material with convective surface flow. The temperature dependent electrical resistance of these sensors is used to measure temperatures, heat flux and heat transfer coefficients [16,12,27]. These sensors provide high accuracy measurements while the spatial resolution is limited by the sensor dimensions. By using infrared thermography, no temperature sensors have to be integrated, since surface temperature is measured by the IR sensor. This reduces the instrumentation effort and offers a high spatial resolution with short response times and a high temperature sensibility.

The present TDT method can be correlated to a class of infrared thermography techniques know as thin skin calorimeter which consist of a thermally thin slab exposed to convective flow. In this case, the slab material is a high emissivity coating layer which is insulated at the back surface. Since a constant temperature over the slab thickness is assumed, local heat transfer is evaluated from the temporal change in slab surface temperature [5,4]. Conventional infrared thermography techniques often suffer from interfering reflections and uncertainties due to insufficiently known emissivities of the coating [13,28,9]. Those effects can cause errors in heat transfer measurements and have to be considered. The present method effectively reduces both interfering reflections and variations in surface coating properties by evaluating relative temperature differences and subtracting a reference measurement without forced convection. This additionally accounts for heat losses due to a non-ideal isolation of the slab for sufficiently low heat transfer coefficients.

In this paper, heat transfer coefficients are derived from transient temperature data and compared to theory. This can be done by developing a model of the heat transfer processes in the slab material and calculate heat transfer coefficients by knowing the specific thermophysical constants. This approach is described by analytical and numerical models of Cook and Felderman [8], Kendall and Dixon [18] and Walker and Scott [29] with applications ranging from short-duration facilities [23] to film cooling experiments [26]. Further improvements of these techniques have been achieved by considering a full inverse analysis of the transient temperature behavior using multi-dimensional

* Corresponding author.
E-mail address: stefan.hoesslin@mtu.de (S. von Hoesslin).

https://doi.org/10.1016/j.expthermflusci.2019.06.004
Received 24 December 2018; Received in revised form 10 May 2019; Accepted 3 June 2019
Available online 11 June 2019
0894-1777/

least-squares minimization [20,2]. However, determining the specific thermo-physical constants can be error-prone and sometimes not possible. As a proof of concept, this work follows a different approach by conducting a calibration measurement which converts TDT data into heat transfer coefficients.

A particular feature of the TDT method is that it uses a pulsed laser for heating up the slab material within nanoseconds. The decay of thermal energy is measured during short periods of time ranging between a few milliseconds to several hundred milliseconds. This allows the application of the technique in setups even when convective conditions are only stable for short durations. Due to short integration times of the camera down to a few microseconds and short heating pulses of the laser (few nanoseconds), periodic flow conditions, like on rotating turbine blades can be examined. Furthermore, heating with a high-power laser provides highly reproducible temperature differences and allows for almost any geometric shapes of the heating area by using diffuser optics with micro-structured surfaces. This is particularly favorable for applications with limited optical accessibility, such as gas turbine parts. The TDT method constitutes a tool that aims for contactless flow visualization and heat transfer measurements in hard-to-access geometries and rotor applications with low instrumentation effort.

In the following, heat conduction processes in the slab material are analyzed to derive a calibration relation theoretically. The relation is confirmed by measurements using Nusselt correlations. It is shown that the calibration relation recorded under specific conditions can be applied to other flow situations and geometries.

2. Measurement principle and theory

2.1. Description of thermodynamic processes during a TDT measurement

The TDT method requires a surface coating with high emissivity which is isolated by a low thermal conductivity layer against the underlying material. By radiating the coated surface with a single-pulsed laser, the topmost layers of the coating are heated up by several degrees.

Right after the pulse, the temperature of the surface declines due to conduction into the material, radiation and convection into the flow. The integral effect of these heat transfer mechanisms is recorded by a high-speed IR camera to determine the dynamics of the temperature decline. A post-processing algorithm is used to calculate the temperature decline rate for every pixel, to achieve a two-dimensional map of quantities proportional to the heat transfer coefficient.

To understand the dynamics of the temperature decline shortly after the heat pulse, a one-dimensional numerical simulation was developed by the authors which was outlined in von Hoesslin et al. [25]. It analyses the heat conduction in a multi-layer system under a constant convection condition and is used here to illustrate the heat transfer processes. For the free-jet experiments in this study only weak temperature gradients in flow direction are present (< 0.1 K between neighboring pixels), such that two-dimensional conduction effects are negligible. However, they become increasingly important for flow conditions where strong temperature gradients are present [11,22].

For the present case the above mentioned two-layer system with aluminum substrate material was simulated. The left-hand side of Fig. 1 shows the temporal behavior of the temperature right after the heat pulse. The simulation was performed for different convection conditions with heat transfer coefficient α varying from 0 to 3000 W/(m^{2}K). The temperature decline rate Λ was calculated from the temporal temperature behavior (Fig. 1, center). Shortly after the heat pulse at t = 0 ms, the heat is conducted from the uppermost molecule layers of the high emissivity coating into the material. This fast process results in a rapid decrease of Λ until the isolation layer strongly reduces further conduction into the underlying aluminum substrate. The heat inside the coating layer now serves as a heat reservoir for the ongoing convection into the flow. A quasi-stationary Λ develops for several milliseconds. By plotting Λ in this time range against the corresponding α (Fig. 1, right-hand side), a quasi-linear relation is observed where TDT data can be correlated to quantitative heat transfer coefficients. Compared to previous simulations and measurements in von Hoesslin et al. [25], different layer materials were used for the current study (see Section 3). In the measurements described in this paper, the quasi-linear relation was confirmed. To motivate the relation theoretically, the quasi-constant state of Λ serves as a necessary prerequisite which is described in the following.

2.2. Theoretical derivation of the calibration relation

In the previous paper, a theory was developed to describe the temperature decline after the heat pulse by assuming the isolation layer beneath the slab material to be ideal [25]. The present paper extents this theory by additionally considering the heat conduction into the substrate material. The assumptions made for this theory lead to a calibration relation which is in agreement with the numerical simulations. After the heat pulse, the temperature decline on the surface takes place due to a combination of heat fluxes including convection into the flow $\dot{q}_{\mathrm{conv}}$ and conduction into the base material $\dot{q}_{\mathrm{cond}}$. Losses due to radiation are negligible, since only small temperature changes are considered.

$$\dot{q} = \dot{q}_{\mathrm{conv}} + \dot{q}_{\mathrm{cond}}. \tag{1}$$

The surface temperature rise $\Delta T_0 = T - T_\infty$ is proportional to the pulse energy q_{pulse} according to the first law of thermodynamics

$$\Delta T_0 = \frac{q_{\mathrm{pulse}}}{C}. \tag{2}$$

Here, $C = c\rho h$ is a proportionality constant containing the specific heat of the slab and the density, while h corresponds to the penetration depth of the thermal wave within the coating. After a short time (typically after 50 ms) quasi-stationary conditions are present as can be seen from the simulation. Here, the spatial slab temperature is almost constant. Using Newton's law of cooling, the resulting differential equation can then be written as

$$\Delta\dot{T} = \frac{1}{C}(\alpha\Delta T + \dot{q}_{\mathrm{cond}}), \tag{3}$$

with α being the convective heat transfer coefficient

$$\alpha = C\frac{\Delta\dot{T}}{\Delta T} - \frac{\dot{q}_{\mathrm{cond}}}{\Delta T}. \tag{4}$$

The term $\Lambda = \Delta\dot{T}/\Delta T$ represents the temperature decline rate which can be extracted from the measured temperature behavior using the numerical representation of$\Delta\dot{T}$. Assuming constant α, Λ can be considered as constant only if $\dot{q}_{\mathrm{cond}}$ is linear with ΔT which is true for small temperature changes present across the slab.

By setting α to zero, a reference measurement without forced convection is performed which is subtracted from the measurement with flow. The temperature decline in this case is governed by natural convection and conduction into the base material

$$\Lambda_{\mathrm{ref}} = \frac{\dot{q}_{\mathrm{cond,ref}}}{C\Delta T_{\mathrm{ref}}} + \alpha_{\mathrm{n}}. \tag{5}$$

Quantities relating to the reference measurement are indexed with "ref", α_{n} is the heat transfer coefficient of natural convection. The reference measurement serves mainly as correction for spurious reflections, inhomogeneous heating and varying coating thicknesses as observed in von Hoesslin et al. [25]. For sufficiently small heat transfer coefficients, it additionally reduces systematical errors due to conduction losses

$$\alpha = C(\Lambda - \Lambda_{\mathrm{ref}}) + \alpha_{\mathrm{n}} + f_{\mathrm{cond}}(\alpha), \tag{6}$$

with $f_{\mathrm{cond}}(\alpha) = (\dot{q}_{\mathrm{cond,ref}}/\Delta T_{\mathrm{ref}} - \dot{q}_{\mathrm{cond}}(\alpha)/\Delta T(\alpha))$. Simulations predict a

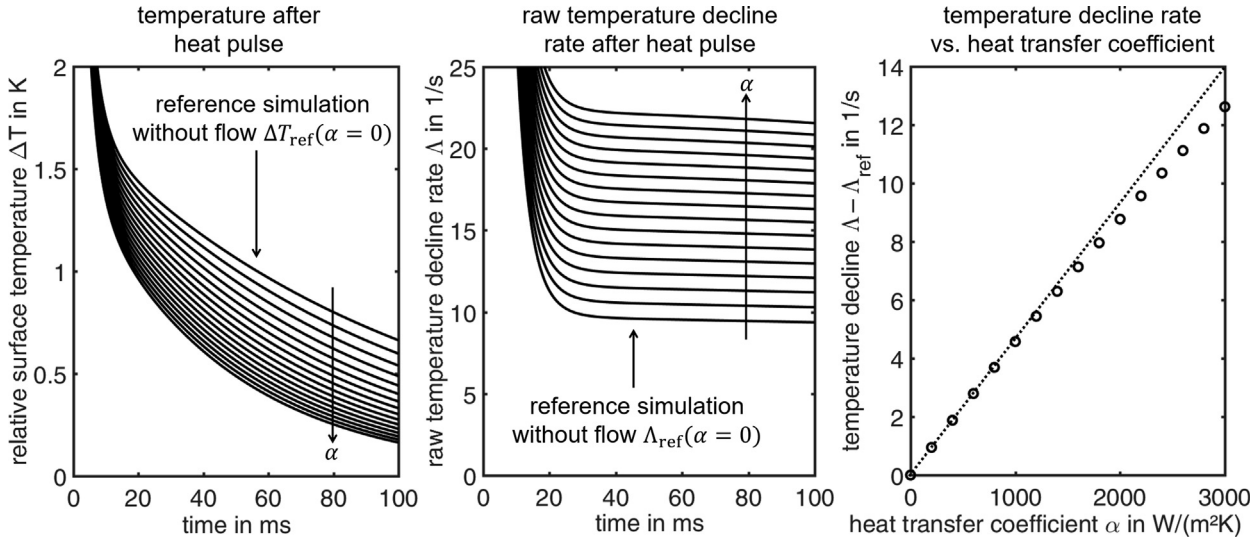

Fig. 1. Left Simulation of the temporal temperature behavior for different heat transfer coefficients $\alpha \in [0, 3000]$ W/(m^{2}K). **Center** Calculated raw temperature decline rates Λ for the same heat transfer coefficients. The temperature decline rate without forced convection ($\alpha = 0$) is defined as Λ_{ref}. **Right** Extraction of the temperature decline $\Lambda - \Lambda_{ref}$ from the quasi-constant time regime at 80 ms from the left-hand plot. A quasi-linear relation between TDT data and heat transfer coefficient is predicted.

linear behavior of $\dot{q}_{cond}(\alpha)/\Delta T(\alpha)$ for small αvalues and thus $f_{cond}(\alpha) \propto \alpha$. This leads to a linear calibration relation which will be used in the following to convert TDT decline rates into heat transfer coefficients

$$\alpha = C'(\Lambda - \Lambda_{ref}) + \alpha_n, \tag{7}$$

with C' containing material parameters and conduction coefficients of the reference measurement. The deviation from linearity of the calibration relation as is observed on the right hand side of Fig. 1, is accounted to the deviation from the linear behavior of $\dot{q}_{cond}(\alpha)/\Delta T(\alpha)$ for large α values.

2.3. Nusselt correlations used for calibration

For a calibration measurement both, α and $\Lambda - \Lambda_{ref}$ must be determined to estimate the proportionality constant C' and the calibration offset. As a proof of concept, α is calculated here using the Nusselt correlations while $\Lambda - \Lambda_{ref}$ is measured by TDT. The valid use of a Nusselt correlation requires a calibration vehicle with defined properties. For this study a flat plate with negligible pressure gradient was used. Literature provides Nusselt correlations for flat plates in static flow for either uniform surface temperature or uniform heat flux within the measurement area. Regarding TDT measurements, approximately uniform surface temperatures are expected across the measurement area. To confirm this assumption, a simulation of the temperature decline was performed following the description in Section 2.1. Fig. 2 shows the calculated convective heat flux extracted at 80 ms after the heat pulse for different heat transfer coefficients. According to the Nusselt correlation heat transfer coefficients can be correlated to the local distance on a flat plate and thus to the simulated changes in surface temperature and heat flux. Fig. 2 shows the variation of both quantities within the first 10% chord length of a flat plate in laminar flow with $Ma = 0.15$ as is used for calibration in the subsequent measurements. It is found, that the convective heat flux and therefore the surface heat flux of the slab material increases by a factor of more than 7.3 across the measurement area while the surface temperature rises by a factor of only 0.4. Shortly after the leading edge the temperature across the measurement area can therefore be considered as uniform.

The simulation implies that for the calibration of TDT measurements, the use of the Nusselt correlation for uniform surface temperature is preferable to the use of the Nusselt correlation for uniform heat flux. For static, laminar flow [17] the Nusselt correlation takes the form

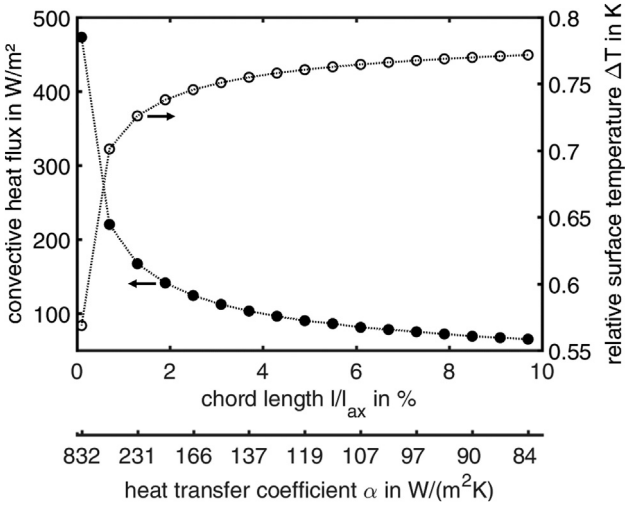

Fig. 2. Simulation of convective heat flux and relative surface temperature for different heat transfer coefficients. A conversion to corresponding locations on a flat plate as is used for calibration experiments is calculated using the Nusselt correlation at a flow velocity of $u = 51$ m/s.

$$\alpha_{lam}(x) = Nu_{x,lam} \cdot \frac{k}{x} = 0.332 \cdot Re_x^{\frac{1}{2}} \cdot Pr^{\frac{1}{3}} \cdot \frac{k}{x}, \tag{8}$$

where x is the distance from the leading edge of the flat plate, $Nu_{x,lam}$ the local Nusselt number in laminar flow, k the thermal conductivity of the fluid, Re_x the local Reynolds number and Pr the Prandtl number. For turbulent flow an empirical correlation is given [17]

$$\alpha_{tur}(x) = Nu_{x,tur} \cdot \frac{k}{x} = 0.0296 \cdot Re_x^{\frac{4}{5}} \cdot Pr^{\frac{1}{3}} \cdot \frac{k}{x}. \tag{9}$$

3. Calibration setup

The calibration measurements were performed on a flat plate at zero angle of attack in a free jet facility. The aluminum plate was laminated with a Kapton isolation foil with a low thermal conductivity of 0.12 W/(mK) according to Dupond [10]. The foil is coated with Nextel-Velvet-

Coating 811-21 which offers a high emissivity of around 0.97 in the spectral range of 2 – 6 µm, see Batuello et al. [3]. The leading edge of the plate has an asymmetrical profile which was derived from a numerical optimization which minimizes the pressure gradient around the leading edge [15]. The plate was positioned in the center of an exit nozzle of the free jet facility with 160 mm diameter at Mach numbers varying from $Ma = 0$ to 0.15.

For the TDT measurement, a high-energy Nd-YAG laser with 5 J pulse energy heats up the coating and 35 ns pulse length at 1064 nm wavelength. The laser beam is expanded by an engineered diffuser, resulting in a homogeneously heated measurement area of about 50 mm × 50 mm. A high-speed infrared camera with InSb detector (Infratec IR9300) is used to record the temperature decline with 200 Hz frame rate within a wavelength range of 2 – 5.7 µm. Both laser and camera were triggered externally to ensure synchronized measurements. The camera acquires 150 frames beginning directly after the heat pulse generated by the laser.

For the calibration, a measurement with flow and a reference measurement without flow were conducted with exactly the same geometry and equipment settings. The data reduction was performed following the steps described in von Hoesslin et al. [25].

Since heat transfer coefficients are equal perpendicular to the flow direction, the resulting image was spatially averaged over 300 pixels to gain the mean profile section of $\Lambda - \Lambda_{ref}$ along the chord of the plate. This profile section was compared to heat transfer coefficients $\alpha(x)$ from the Nusselt correlation by calculating the corresponding x and Re_x for each pixel along the chord line and applying Eqs. (8) and (9) to derive $\alpha(x)$.

4. Results and discussion

4.1. Calibration measurements

For the calibration measurements, the free-jet was set to three different flow velocities, 17 m/s, 33 m/s and 51 m/s resulting in different Re_x ranges along the plate. A laminar boundary layer developed within the first centimeters of the flat plate. The measurement area started at the leading edge of the plate within the laminar region. For this measurement area and free-jet velocities, a local Reynold's number range of $Re_x \in [0.32 \cdot 10^3, 155 \cdot 10^3]$ was achieved for calibration. By using the local Nusselt correlation for laminar flow Eq. (8), heat transfer coefficients $\alpha(x)$ were calculated along the plate.

By plotting $\alpha(x)$ against the measured TDT signal $\Lambda - \Lambda_{ref}$, a linear calibration relation can be observed as is shown in Fig. 3. Datasets of three different free-jet velocities were fitted using a linear regression resulting in the calibration relation

$$\alpha = 227.3 \frac{\mathrm{Ws}}{\mathrm{m^2K}} (\Lambda - \Lambda_{ref}) + 13.5 \frac{\mathrm{W}}{\mathrm{m^2K}}, \tag{10}$$

where the calibration constant is determined to $C' = 227.3 \pm 1.5$ Ws/(m^{2}K). The measurements suggest that the described theoretical model in Section 2.2 is applicable and that TDT data can be converted into heat transfer coefficients by applying the calibration relation within $\alpha = 50 - 500$ W/(m^{2}K). This confirms the assumption, that within this range $f_{cond}(\alpha)$ in Eq. (6) can be approximated as linear in α. It thus affects only gradient and offset of the calibration relation.

The offset of 13.5 ± 0.8 W/(m^{2}K) at $\Lambda - \Lambda_{ref} = 0$ is explained by natural convection being present during the reference measurement without forced convection. This lies within the order of magnitude predicted by a correlation for natural convection on horizontal plates in air [7].

The uncertainties given for the offset and calibration constant were derived from the fit. The total error of this setup consists of systematical and statistical errors of the TDT method as well as the uncertainty due to the calibration relation. The latter is not negligible when applying the Nusselt correlation in non-ideal flow conditions. In this study, using the Nusselt correlation for calibration serves as proof-of-concept which demonstrates that in principle TDT data are linear with changing heat transfer coefficients. Using a second, well-established measurement technique for calibration instead, the error due to the calibration method can be reduced and specified. The statistical uncertainty of the TDT method, on the other hand, is determined by factors like the heating temperature, coating and used optics which specify the available light and the resulting signal-to-noise ratio of the IR-sensor. Spatial and temporal averaging has to be applied to enhance data quality which is thus dependent on the given measurement situation and required spatial resolution. For the current calibration measurement, the pixel-wise statistical uncertainty in flow direction is approximately $\Delta(\Lambda - \Lambda_{ref}) = 0.03$ 1/s or expressed in heat transfer coefficient, $\Delta\alpha = 6.8$ W/(m^{2}K) using Gaussian error propagation.

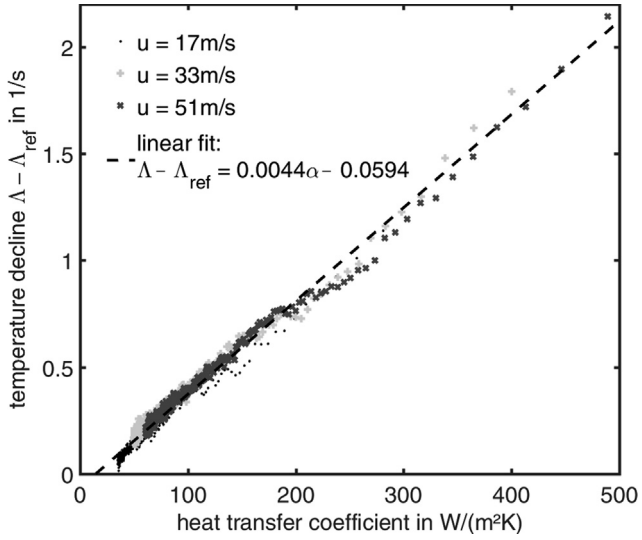

Fig. 3. Linear calibration relation between data measured by Temperature Decline Thermography (TDT) and heat transfer coefficients calculated by the Nusselt correlation for different exit velocities u of the free-jet. A linear regression (dashed line) was fitted to the data of all free-jet velocities.

It is emphasized, that the calibration relation in Eq. (10) is only valid if the same set of measurement and analysis parameters are used. This contains the camera integration time, the used lens, the time interval on the temperature transient used for analysis, as well as heating temperature, type and thickness of the coating. Changes in these parameters will lead to systematical uncertainties when using the given calibration relation. Since only relative temperatures are measured, parameters like sample frequency and heating temperatures have a primarily negligible influence on calibration which is considered small compared to the statistical uncertainty of the method. However, for high heating temperatures the amount of heat emitted into the boundary layer is not negligible. Especially in laminar flows, the convection into the flow can thereby be reduced towards downstream areas resulting in an altered calibration relation. This effect depends on flow velocity and type of fluid. For the present measurements a heating temperature of about 10 K was observed to have negligible influence on the calibration relation.

However, other parameters like the time interval on the temperature transient used for analysis, thickness and type of the coating are expected to have an influence on calibration. In order to transfer the calibration to other measurements, these parameters have to be kept constant for calibration and measurement. The analysis interval can be kept constant for most applications. Further effort is needed to determine the sensitivity of the calibration to changes in coating.

Another group of parameters often cannot be kept constant for calibration and measurement but have negligible influence on calibration. This includes camera angle and distance from the object. Different

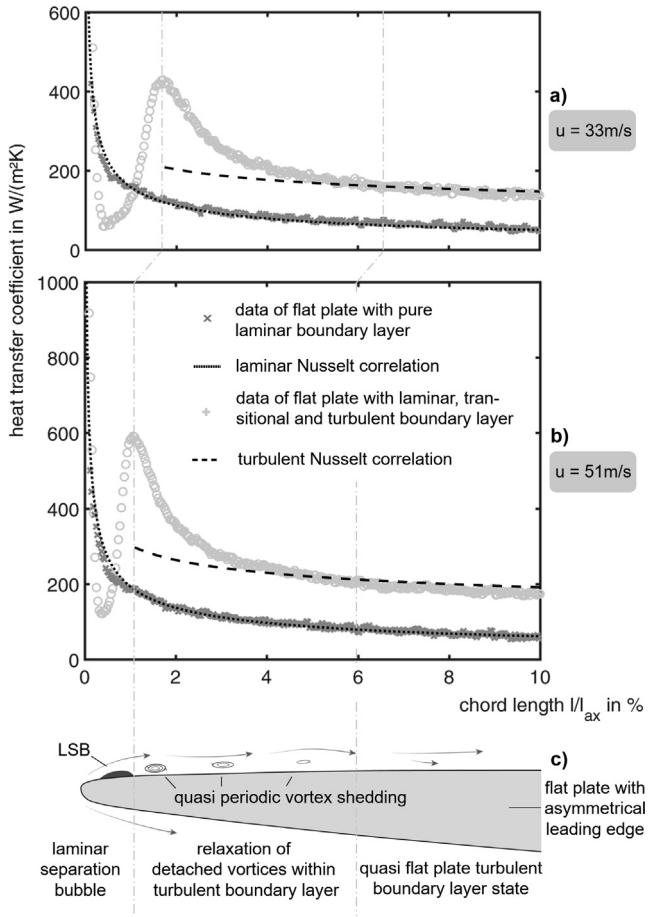

Fig. 4. (a) and (b) show TDT data recorded in a laminar boundary layer as dark grey crosses which correspond to the data of u= 33 m/s and u= 51 m/s shown in Fig. 3. Additionally, data measured in a transitional and turbulent boundary layer on an inclined plate are shown as light grey circles. Both datasets were converted to heat transfer coefficients using the calibration relation Eq. (10). For comparison, the Nusselt correlation for laminar and turbulent flow are shown as dotted and dashed lines. The schematic in (c) shows the transitional and turbulent flow around the leading edge of the inclined plate. The laminar-turbulent transition, visible within the first millimeters of the plate, is triggered by a laminar separation bubble which is associated with quasi periodic vortex generation after reattachment of the flow. The vortices disperse gradually until a flat plate turbulent boundary layer state is observed.

camera angles (0 – 70° from the surface normal) and distances (0.5 – 1.0 m) with respect to the coated surface have been tested with negligible influence on the TDT signal (less than 1%). This allows the calibration to be applied to data of different geometric arrangements.

4.2. Transfer of the calibration relation to turbulent flow conditions

The aim of the following experiments is to show the possibility of transferring a calibration relation recorded under known conditions to other flow situations and geometries. Since the received calibration constants are independent of the flow condition, the calibration relation recorded in laminar flow also applies to other flow conditions.

To verify this, the flat plate was inclined by 4° to force a laminar separation bubble to occur and a laminar-turbulent transition near the leading edge on the upper side of the plate. A TDT measurement was performed and the data were converted to heat transfer coefficients using Eq. (10). By comparing the resulting data of the turbulent flow to the corresponding Nusselt correlation Eq. (9), the validity of applying the calibration relation recorded in laminar flow to a turbulent flow situation is confirmed.

In Fig. 4(a) and (b), the local TDT data of the calibration measurement is shown as dark grey crosses along the chord line of the plate. This dataset corresponds to the data of Fig. 3 at u = 33 m/s and u = 51 m/s respectively which were converted to heat transfer coefficients using Eq. (10). For the sake of completeness, the laminar Nusselt correlation which was used for calibration is shown as well, see black dotted line. The decreasing heat transfer with increasing boundary layer thickness and local Reynolds number is expected as the flow velocity gradient at the wall decreases with increasing boundary layer thickness.

The dataset of the inclined plate is shown in light grey circles. The data was converted to heat transfer coefficients using the same calibration relation Eq. (10). At u = 51 m/s (Fig. 4(b)), a characteristic change from low to high heat transfer coefficients is observed within the first six millimeters from the leading edge, corresponding to a laminar-turbulent transition. After the transition, a turbulent boundary layer develops which results in a gradual decrease of heat transfer coefficients. The laminar-turbulent transition is taking place in the shear layer of a laminar separation bubble. Due to the lack of fluid movement within the laminar separation bubble [21], the heat transport is reduced resulting in lower heat transfer coefficients than in the laminar boundary layer. The subsequent increase marks the end of the laminar separation bubble where the flow reattaches and more heat is carried away due to the turbulent flow state after reattachment. The reattachment is a dynamic process. Small vortices develop at the end of the bubble which are detaching in an oscillating manner known as vortex shedding [14]. This process is sketched in the schematic of Fig. 4(c).

This results in higher mean heat transfer coefficients compared to the predictions of the turbulent Nusselt correlation for flat plates (black dashed line). The detached vortices gradually disperse in the turbulent flow and a flat plate similar boundary layer develops after about three centimeters. An asymptotic approach to the turbulent Nusselt correlation is observed within the last three centimeters of the measurement area. Within this range, it is shown that the calibration relation recorded in laminar flow can be validly applied to a measurement in turbulent flow with constant measurement parameters and different geometric setups.

5. Conclusion

The analysis conducted in this paper has four important implications:

1. It was shown that data recorded by the TDT method can be correlated to heat transfer coefficients by a linear calibration relation. This confirms the developed theory of the temporal temperature decline and the numerical simulations based on the heat equation.
2. The calibration relation recorded in laminar flow can be used to convert data measured in turbulent flow into quantitative heat transfer coefficients. Good agreement to the corresponding Nusselt correlation was observed. Constraints to the application of the calibration to measurements in other flow conditions and geometries were given.
3. With a quantitative representation of TDT data, laminar and turbulent boundary layer conditions can be characterized. Furthermore different flow states like laminar separation bubbles can as well be classified and analyzed.
4. The use of the Nusselt correlation showed that calibration of TDT data is in principal possible. In future experiments however, it would be reasonable to replace the correlation by a second measurement technique. The error of the calibration relation can then be defined more precisely. Simulations showed that it is preferable to use a technique that measures heat transfer coefficients by means of a uniform surface temperature rather than a uniform heat flux.

The TDT method is capable of detecting laminar-turbulent transition qualitatively in hard-to-access geometries. Combined with the possibility to obtain quantitative heat transfer, the technique is beneficial for a range of high-speed applications where a two-dimensional overview of the flow situation, but also detailed quantitative information are required.

Declaration of Competing Interest

The authors declared that there is no conflict of interest.

Acknowledgements

This research was partially supported by the cooperative project COOREFLEX-turbo.

References

[1] T. Astarita, G.M. Carlomagno, Infrared Thermography for Thermo-Fluid-Dynamics, Springer, Berlin, Heidelberg, 2013.
[2] F. Avallone, A low–computational–cost inverse heat transfer technique for convective heat transfer measurements in hypersonic flows, Exp. Fluids 56 (2015) 86.
[3] M. Batuello, S. Clausen, J. Hameury, P. Bloembergen, The spectral emissivity of surface layers, currently applied in blackbody radiators, covering the spectral range from 0.9 to 20 μm. An International Comparison. Tempmeko, 1999, pp. 601–606.
[4] D. Bougeard, Infrared thermography investigation of local heat transfer in a plate fin and two-tube rows assembly, Int. J. Heat Fluid Flow (2007) 988–1002.
[5] R. Boutarfa, S. Harmand, Local convective heat transfer for laminar and turbulent flow in a rotor-stator system, Exp. Fluids (2005) 209–221.
[6] G. Carlomagno, L. de Luca, G. Cardone, T. Astarita, Heat flux sensors for infrared thermography in convective heat transfer, Sensors (2014) 21065–21116.
[7] T. Chen, H. Tien, B. Armaly, Natural convection on horizontal, inclined, and vertical plates with variable surface temperature or heat flux, Int. J. Heat Mass Transf. (1986) 1465–1478.
[8] W. Cook, E. Felderman, Reduction of data from thin-film heat-transfer gages - A concise numerical technique, AIAA J. (1966) 561–562.
[9] B.K. Crawford, G.T. Duncan Jr, D.E. West, W.S. Saric, Laminar-turbulent boundary layer transition imaging using IR thermography, Opt. Photon. J. (2013) 233.
[10] Dupont, http://www.dupont.com. Retrieved from http://www.dupont.com/content/dam/dupont/products-and-services/membranes-and-films/polyimde-films/documents/DEC-Kapton-summary-of-properties.pdf, 23. May 2018 (Accessed: 10. May 2019).
[11] M. Estorf, Image based heating rate calculation from thermographic data considering lateral heat conduction, Int. J. Heat Mass Transf. (2006) 2545–2556.
[12] G. Fralick, J. Wrbanek, C. Blaha, Thin film heat flux sensor of improved design, Proceedings of NASA Technical Memorandum (S. 1-14), NASA, Washington, 2002.
[13] E. Gartenberg, R.E. Wright, Boundary-layer transition detection with infrared imaging emphasizing cryogenic applications, AIAA J. (1994) 1875–1882.
[14] R. Hain, C.J. Kähler, R. Radespiel, Dynamics of laminar separation bubbles at low-Reynolds-number aerofoils, J. Fluid Mech. (2009) 129–153.
[15] R.E. Hanson, H.P. Buckley, P. Lavoie, Aerodynamic optimization of the flat-plate leading edge for experimental studies of laminar and transitional boundary layers, Exp. Fluids (2012) 863–871.
[16] F. Haselbach, W. Nitsche, Calibration of single-surface hot films and in-line hot-film arrays in laminar or turbulent flows, Meas. Sci. Technol. (1996) 1428–1438.
[17] F. Incropera, D. De Witt, Fundamentals of Heat and Mass Transfer, Wiley, New York, 1985.
[18] D.N. Kendall, W. Dixon, Heat transfer measurements in a hot shot wind tunnel, Trans. Aerospace Electronic Syst. (1996) 596–603.
[19] H. Mocikat, H. Herwig, Heat transfer measurements with surface mounted foil-sensors in an active mode: A comprehensive review and a new design, Sensors (2009) 3011–3032.
[20] D. Modenini, F.F.J. Schrijer, Heat transfer measurements in a supersonic wind tunnel through inverse temperature data reduction: application to a backward facing step, Quantit. Infrared Thermography (2012) 209–230.
[21] M. Ol, B. McCauliffe, E. Hanff, U. Scholz, C.J. Kähler, Comparison of laminar separation bubble measurements on a low Reynolds number airfoil in three facilities, 35th AIAA Fluid Dynamics Conference and Exhibit,(S. 5149), (2005).
[22] F.F.J. Schrijer, Unsteady data reduction techniques for QIRT: consideration of temporal and spatial resolution, 11th QIRT Conference (S. 317), QIRT, Naples, Italy, 2012.
[23] E. Schülein, Skin-friction and heat flux measurements in shock/boundary-layer interaction flows, AIAA J. (2006) 1732–1741.
[24] M. Stadlbauer, J. Gründmayer, F. von Plehwe, Patentnr, WO2014198251 A1, 2014.
[25] S. von Hoesslin, M. Stadlbauer, J. Gruendmayer, C.J. Kähler, Temperature decline thermography for laminar–turbulent transition detection in aerodynamics, Exp. Fluids (2017) 129.
[26] M.K. Yadav, S.K. Singh, A. Parwez, S. Khandekar, Inverse models for transient wall heat flux estimation based on single and multi-point temperature measurements, Int. J. Therm. Sci. (2018) 307–317.
[27] A. Zribi, M. Barthès, S. Bégot, F. Lanzetta, J.Y. Rauch, V. Moutarlier, Design, fabrication and characterization of thin film resistances for heat flux sensing application, Sens. Actuat. A: Phys. (2016) 26–39.
[28] S. Zuccher, W. Saric, Infrared thermography investigations in transitional supersonic boundary layers, Exp. Fluids (2008) 145–157.
[29] D. Walker G., E. Scott P., Evaluation of estimation methods for high unsteady heat fluxes from surface measurements, Journal of Thermophysics and Heat Transfer (1998) 543–551.